Conclusions

Ab_2Be and AbCpBe help to solve some of the remaining problems in the structural and electronic behavior of beryllocene. The fact that Ab_2Be forms diastereoisomers enables the observation of ring flips in solution. The more stable AbCpBe shows a remarkable conductivity in THF, supporting the suggested dissociation. This is a condition for the observed flip. NMR studies of the mixed complex additionally show that the Cp ring dissociates whereas the Ab ligand remains η^1-coordinated.

It seems reasonable to apply this knowledge to beryllocene. Consequently, Cp_2Be in solution should exist in an equilibrium with $CpBe^+$ and Cp^-. The rate of dissociation depends on the solvent. The fact that in AbCpBe the η^5-bonded Cp ring dissociates whereas the Ab ring remains η^1-bonded shows that the η^1-coordination is stronger than the η^5-coordination. It agrees with the ^{1}H NMR results that only at about +90 °C half of the molecules show η^5-coordinated Ab rings. The result that the ^{1}H NMR spectra of AbCpBe at higher temperatures show separated η^5- and η^1-coordinated Ab rings proves a temperature-dependent equilibrium of two species. So, an oscillation of beryllium is to be excluded. Concerning Ab_2Be and Cp_2Be it can be concluded that also in these compounds two η^5-coordinated rings exist instead of an oscillation of Be between η^5- and η^1-coordinated rings.

Registry No. Ab_2Be (BN/NB), 106420-41-1; Ab_2Be (BN/BN), 106420-42-2; AbCpBe, 106420-43-3; AbLi, 84356-32-1; Cp_2Be, 12083-43-1.

Supplementary Material Available: Tables of atom coordinates, hydrogen atom coordinates, anisotropic temperature factors, bond lengths, and bond angles (5 pages); a listing of structure factor amplitudes (18 pages). Ordering information is given on any current masthead page.

$Ph_2AsCH_2CH_2PPh_2$ (arphos) and $Ph_2PCH_2CH_2PPh_2$ (diphos) Complexes of $Co_2(CO)_6MCCO_2$-*i*-Pr [M = $Co(CO)_3$, $(C_5Me_5)Mo(CO)_2$]: X-ray Crystal Structure and NMR Fluxionality

Karen A. Sutin,[†] Joseph W. Kolis,[†] Michael Mlekuz,[†] Peter Bougeard,[†] Brian G. Sayer,[†]
Michael A. Quilliam,[†] Romolo Faggiani,[‡] Colin J. L. Lock,[‡] Michael J. McGlinchey,*[†] and
Gérard Jaouen*[§]

Department of Chemistry and Institute for Materials Research, McMaster University,
Hamilton, Ontario, L8S 4M1, Canada, and Ecole Nationale Supérieure de Chimie, 75231 Paris Cedex, France

Received November 18, 1985

The tetrahedral clusters $Co_2(CO)_6MCR$, where R = CO_2CHMe_2 and M = $Co(CO)_3$ or $(C_5Me_5)Mo(CO)_2$, react with $Ph_2PCH_2CH_2PPh_2$ (diphos) and $Ph_2AsCH_2CH_2PPh_2$ (arphos). The molecule $Co_3(CO)_7$(arphos)CR crystallizes in space group *Pbca* with a = 17.845 (4) Å, b = 19.630 (4) Å, c = 22.426 (3) Å, and Z = 8. The structure has been solved by direct and Fourier methods and refined by full-matrix least squares to R_1 and R_2 values of 0.075 and 0.092, respectively, for 2317 observed reflections. The structure reveals that the arphos ligand spans equatorial positions on adjacent cobalts, thus forming a six-membered ring in a half-chair conformation. ^{1}H and ^{13}C NMR studies show that, in the Co_3(arphos) complex, the molecule loses its stereochemical integrity via migration of the arsenic terminus between cobalt atoms. In contrast, the Co_3(diphos) system and both of the Co_2Mo complexes retain their configurations. However, the $(C_5Me_5)Mo(CO)_2$ vertex can rotate with respect to the cluster, and two orientations are detectable at low temperature. Concomitantly, carbonyl migrations occur and the various mechanistic possibilities are discussed.

Introduction

With the ultimate goal of using organo-transition-metal clusters in asymmetric catalysis,[1] attention has been focused on synthetic routes to chiral clusters.[2] Among the plethora of systems now available are those in which each vertex of the polyhedron bears a different transition metal or main group element. Nevertheless, molecules such as 1 and 2, which fulfill the classic criteria for chirality, exhibit fluxional behavior and so racemize even on the NMR time scale.

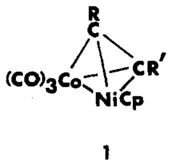

1

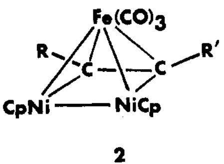

2

[†] Department of Chemistry, McMaster University.
[‡] Institute for Materials Research, McMaster University.
[§] Ecole Nationale Supérieure de Chimie.

(1) Bosnich, B. *Chem. Brit.* 1984, *20*, 808. (b) Pittman, C. U., Jr.; Richmond, M. G.; Absi-Halabi, M.; Beurich, H.; Richter, F.; Vahrenkamp, H. *Angew. Chem., Int. Ed. Engl.* 1982, *21*, 786.

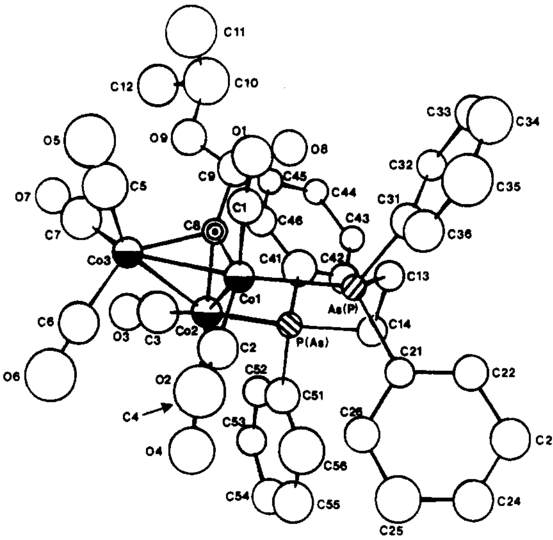

Figure 1. ORTEP diagram of $Co_3(CO)_7(arphos)CCO_2CHMe_2$ (4).

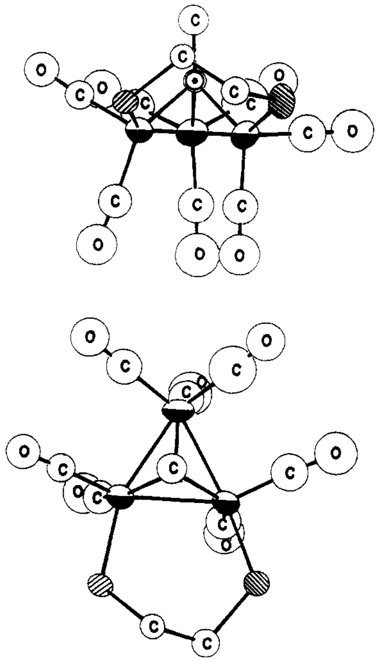

Figure 2. ORTEP diagrams of 4 with the phenyl rings and the ester functionality removed for clarity: (a) view in the tricobalt plane showing the half-chair conformation of the chelate ring; (b) view down the pseudothreefold axis showing the equatorial orientation of the arphos ligand and the twisting of the carbonyl groups.

Table I. Crystal Data

compd	$C_{38}H_{31}AsCo_3P$
fw (daltons)	914.4
cryst size, mm	0.25 × 0.35 × 0.10
systematic absences	$0kl$, $k = 2n + 1$, $h0l$, $l = 2n + 1$, $hk0$, $k = 2n + 1$
space group	$Pbca$ (No. 61)
unit cell	
a, Å	17.845 (4)
b, Å	19.630 (4)
c, Å	22.426 (3)
V, Å^3	7856 (3)
Z	8
ρ_{calcd}, g/cm^3	1.546
ρ_{obsd}, g/cm^3	1.53 (2)
temp, °C	22
linear abs coeff μ, cm^{-1}	22.47
no. of reflctns measd	7436
no. of independent reflctns	4354
R_{merg}	0.026
max 2θ reflctns measd	45°, $h,k,\pm l$
no. with $I > 3\sigma$	2317
std reflctns (esd, %)	2,−8,4 (0.012), 0,6,−4 (0.012)
final R_1, R_2^{a} for $I > 0$	0.138, 0.146
final R_1, R_2^{a} for $I > 3\sigma$	0.075, 0.092
final shift/error, max (av)	0.014 (0.003)
χ (secondary extinction)	0.000 11
final diff map max peak (valley), e Å^3	1.1, −1.0
weighting scheme	$w = (\sigma_F^2 + 0.005\,39F_o^2)^{-1}$
error in an observn of unit wt	1.34

[a] $R_1 = (\sum||F_o| - |F_c||/\sum|F_o|)$; $R_2 = [\sum w(|F_o| - |F_c|)^2/\sum wF_o^2]^{1/2}$.

A synthetically less demanding route to chiral clusters involves the incorporation of unsymmetrical bidentate ligands. Such ligands can render chiral the readily available $RCCo_3(CO)_9$ clusters whose chemistry has been exhaustively studied, notably by Seyferth[3] and by Robinson.[4] We here describe the synthesis and characterization of a series of such molecules; some of these complexes do not retain their stereochemical integrity even on the NMR time scale and their mechanisms of rearrangement are examined.

Results and Discussion

Carbynyl clusters of the $RCCo_3(CO)_9$ type can be prepared in a high-yield one-step synthesis, and, furthermore, the replacement of a $Co(CO)_3$ vertex by isolobal fragments such as CpNi or $CpMo(CO)_2$ is a facile process.[5] Treatment of these compounds with a bidentate ligand, e.g., $Ph_2PCH_2CH_2PPh_2$ (diphos), leads to replacement of two carbonyls and formation of a chelate ring. When the bidentate ligand is unsymmetrical, e.g., $Ph_2PCH_2CH_2AsPh_2$ (arphos), the molecule is chiral. Consequently, the series of molecules 3 through 6 were prepared via the reactions

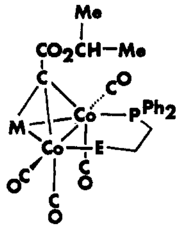

3 M = $Co(CO)_3$; E = PPh_2
4 M = $Co(CO)_3$; E = $AsPh_2$
5 M = $(C_5Me_5)Mo(CO)_2$; E = PPh_2
6 M = $(C_5Me_5)Mo(CO)_2$; E = $AsPh_2$

of the appropriate clusters with diphos or arphos. The structure of one molecule in the series was established X-ray crystallographically, and it is immediately apparent from the ORTEP diagrams in Figures 1 and 2 that two equatorial carbonyl ligands have been replaced. In previous structural determinations on monosubstituted $RCCo_3(CO)_8PR_3$ complexes, an equatorial carbonyl was likewise replaced;[6] furthermore, carbonyl bridging was

---

(2) (a) Johnson, B. F. G., Ed. *Transition Metal Clusters*; Wiley-Interscience: New York, 1980. (b) Vahrenkamp, H. *Adv. Organomet. Chem.* **1983**, *22*, 169. (c) Tachikawa, M.; Muetterties, E. L. *Prog. Inorg. Chem.* **1981**, *28*, 203. (d) Gladfelter, W. L.; Geoffroy, G. L. *Adv. Organomet. Chem.* **1980**, *18*, 207.

(3) Seyferth, D. *Adv. Organomet. Chem.* **1976**, *14*, 97.

(4) (a) Penfold, B. R.; Robinson, B. H. *Acc. Chem. Res.* **1973**, *6*, 73. (b) Downard, A. J.; Robinson, B. H.; Simpson, J. *Organometallics* **1986**, *5*, 1122; 1132; 1140.

(5) (a) Beurich, H.; Vahrenkamp, H. *Angew. Chem., Int. Ed. Engl.* **1981**, *20*, 98. (b) Mlekuz, M.; Bougeard, P.; McGlinchey, M. J.; Jaouen, G. *J. Organomet. Chem.* **1983**, *253*, 117. (c) Jensen, S.; Robinson, B. H.; Simpson, J. *J. Chem. Soc., Chem. Commun.* **1983**, *1081*.

observed, as in 7, and this was rationalized in terms of the greater σ-donating character of the phosphine ligands. In contrast, when a diarsacyclobutene coordinates, as in 8, it binds at the axial positions.[7]

In the present molecule 4, the chelate ring adopts a "cyclohexene-like" half-chair conformation that, even in the case of a symmetrical bidentate ligand, would destroy the molecular mirror plane and lower the point group from C_s to C_1. The significance of this point will become apparent presently. In 4, the phosphine–arsine is disordered, but the disorder is not complete. That is to say there is not a 50:50 distribution on the As(P) and P(As) positions. The uneven distribution is reflected in the small differences in bond lengths and angles (see Tables II and III). Interestingly, the observed Co–E distances (2.273 (3) and 2.229 (3) Å) are between those observed for a bidentate arsine (2.337 (1) and 2.358 (1) Å)[7] and a tridentate phosphine (2.207 (3) Å)[8] in similar systems.

It should be noted that the quality of the single crystal used for structure determination was not especially high. This along with the disorder problem resulted in rather high agreement factors (see Experimental Section). However, the solution was sufficient to determine the gross geometrical aspects of the molecule.

Despite these factors, the carbon atoms of the bridging methylene groups are well-defined. Both the phosphorus and arsenic atoms, and thus the ethylene carbons of the bridge, are on the same side of the plane defined by the three cobalt atoms and lie proximally to the capping carbyne unit. This fact, coupled with the twist in the bridging ethylene group and the steric requirements of the phenyl groups, causes the carbonyl groups to move so as to destroy the mirror symmetry of the $Co_3(CO)_7$ moiety and introduce a pseudo-C_3 distortion of the carbonyl groups (see Figure 2b). It is interesting that the Co–Co bond bridged by the arphos ligand is significantly longer (2.500 Å) than the other two Co–Co bonds (2.464 and 2.473 Å). Also, the capping alkylidyne carbon is not centrally positioned with respect to the metal triangle; it is, in fact, displaced toward the chelated cobalt atoms. It is noteworthy that a very recent structural study on the analogous bis(diphenylphosphino)methane complex 9 showed very similar features except that the chelate ring adopted the envelope conformation and so retained a molecular mirror plane.[9] In both 4 and 9, all seven carbonyl ligands are clearly terminal.

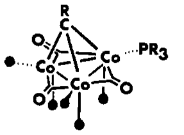

7

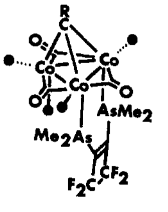

8

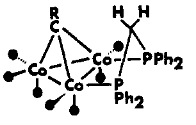

9

Table II. Atomic Positional Coordinates (×10⁴) and Temperature Factors (×10³ Å²)

	x	y	z	U_{eq}[a] or U_{iso}
Co(1)	1368 (1)	1761 (1)	4023 (1)	38 (1)[a]
Co(2)	951 (1)	2236 (1)	3043 (1)	40 (1)[a]
Co(3)	85 (1)	1547 (1)	3650 (1)	44 (1)[a]
As(P)[b]	2627 (1)	1873 (1)	3909 (1)	34 (2)[a]
P(As)[b]	1916 (2)	2440 (1)	2439 (1)	50 (5)[a]
C(1)	1440 (9)	1031 (8)	4464 (7)	48 (4)
C(2)	1160 (11)	2402 (10)	4558 (8)	65 (3)
C(3)	322 (13)	2297 (10)	2489 (10)	83 (6)
C(4)	877 (11)	3052 (11)	3378 (19)	73 (6)
C(5)	−86 (11)	853 (11)	4117 (9)	74 (6)
C(6)	−407 (12)	2245 (11)	3948 (8)	73 (6)
C(7)	−513 (11)	1233 (10)	3068 (9)	135 (7)
C(8)	1053 (8)	1342 (2)	3316 (6)	31 (4)
C(9)	1283 (10)	690 (8)	3057 (7)	53 (5)
C(10)	905 (15)	−282 (13)	2404 (12)	111 (8)
C(11)	746 (14)	−800 (14)	2852 (12)	116 (9)
C(12)	265 (19)	−248 (16)	1935 (14)	157 (12)
C(13)	3080 (8)	1824 (7)	3116 (6)	36 (4)
C(14)	2894 (9)	2462 (8)	2752 (7)	47 (4)
C(21)	3109 (8)	2685 (7)	4172 (7)	40 (4)
C(22)	3867 (10)	2673 (9)	4312 (8)	60 (5)
C(23)	4267 (11)	3291 (10)	4424 (8)	72 (6)
C(24)	3869 (11)	3890 (10)	4433 (8)	68 (5)
C(25)	3087 (12)	3919 (11)	4305 (9)	78 (6)
C(26)	2705 (10)	3301 (9)	4184 (7)	56 (5)
C(31)	3191 (9)	1184 (8)	4309 (7)	50 (5)
C(32)	3462 (12)	631 (11)	4004 (9)	83 (6)
C(33)	3854 (12)	112 (11)	4348 (10)	87 (6)
C(34)	3953 (13)	194 (11)	4936 (10)	86 (7)
C(35)	3691 (12)	753 (11)	5225 (10)	87 (7)
C(36)	3288 (10)	1243 (9)	4920 (8)	59 (5)
C(41)	2040 (9)	1854 (8)	1771 (7)	48 (4)
C(42)	2627 (11)	2014 (9)	1370 (8)	64 (5)
C(43)	2751 (11)	1587 (10)	877 (9)	72 (6)
C(44)	2269 (13)	1031 (11)	794 (10)	89 (7)
C(45)	1698 (16)	899 (14)	1189 (12)	118 (9)
C(46)	1571 (11)	1324 (9)	1705 (8)	63 (5)
C(51)	1828 (9)	3290 (8)	2081 (7)	48 (4)
C(52)	1516 (10)	3334 (9)	1505 (8)	64 (5)
C(53)	1416 (13)	3976 (12)	1237 (10)	95 (7)
C(54)	1659 (13)	4574 (11)	1553 (10)	88 (7)
C(55)	1961 (12)	4506 (11)	2107 (10)	87 (7)
C(56)	2066 (11)	3858 (10)	2378 (9)	72 (6)
O(1)	1525 (7)	542 (6)	4727 (5)	70 (4)
O(2)	996 (8)	2758 (8)	4931 (7)	97 (5)
O(3)	−97 (9)	2344 (8)	2076 (7)	108 (5)
O(4)	808 (8)	3600 (8)	3580 (6)	97 (5)
O(5)	−213 (8)	392 (7)	4408 (6)	89 (4)
O(6)	−693 (9)	2737 (9)	4161 (7)	113 (5)
O(7)	−906 (8)	1000 (7)	2706 (6)	88 (4)
O(8)	1911 (7)	460 (6)	3059 (5)	68 (4)
O(9)	726 (6)	356 (6)	2780 (5)	60 (3)

[a] $U_{eq} = {}^1/_3(U_{11} + U_{22} + U_{33})$. [b] The occupancies of the As(P) position were 0.7136 As and 0.2864 P and/or the P(As) position were 0.7136 P and 0.2864 As.

As part of the characterization of the clusters, their electron-impact mass spectra were recorded but, not surprisingly, showed only fragment ions and a large peak for the phosphine itself. Recent advances in mass spectrometry have included the development of techniques for handling involatile high molecular weight complexes.[10] Some particularly fine recent examples have demonstrated the applicability of the fast atom bombardment (FAB) technique to metal clusters.[11] The FAB method also gives spectacular results with the molecules 3 through 6. Typically, we show a section of the FAB mass spectrum of 5 in which the isotope distribution pattern is clearly resolved. Interestingly, the highest mass peak is for the MH^+ rather

---

(6) (a) Dawson, P. A.; Robinson, B. H.; Simpson, J. *J. Chem. Soc., Dalton Trans.* **1979**, 1762. (b) With an extremely bulky ligand, viz., tricyclohexylphosphine, an axial carbonyl is replaced: Matheson, T. W.; Penfold, B. R. *Acta Crystallogr., Sect. B: Struct. Crystallogr. Cryst. Chem.* **1977**, *B33*, 1980.

(7) (a) Crow, J. P.; Cullen, W. R. *Inorg. Chem.* **1971**, *10*, 2165. (b) Einstein, F. W. B.; Jones, R. D. G. *Inorg. Chem.* **1972**, *11*, 395.

(8) Darensbourg, D. J.; Zalewski, D. J.; Delord, T. *Organometallics* **1984**, *3*, 1210.

(9) (a) Balavoine, G.; Collin, J.; Bonnet, J. J.; Lavigne, G. *J. Organomet. Chem.* **1985**, *280*, 429. (b) In contrast, the diphos ligand in $HRuCo_3(CO)_{10}$(diphos) is diaxially coordinated to two cobalts: Pursiainen, J.; Pakkanen, T. A. *J. Organomet. Chem.* **1986**, *309*, 187.

(10) Miller, J. M. *J. Organomet. Chem.* **1983**, *249*, 299.

(11) (a) Braga, D.; Henrick, K.; Johnson, B. F. G.; Lewis, J.; McPartlin, M.; Nelson, W. J. H.; Sirone, A.; Vargas, M. D. *J. Chem. Soc., Chem. Commun.* **1983**, 1131. (b) Johnson, B. F. G.; Lewis, J.; McPartlin, M.; Raithby, P. R.; Nelson, W. J. H.; Sirone, A.; Vargas, M. D. *J. Chem. Soc., Chem. Commun.* **1983**, 1476.

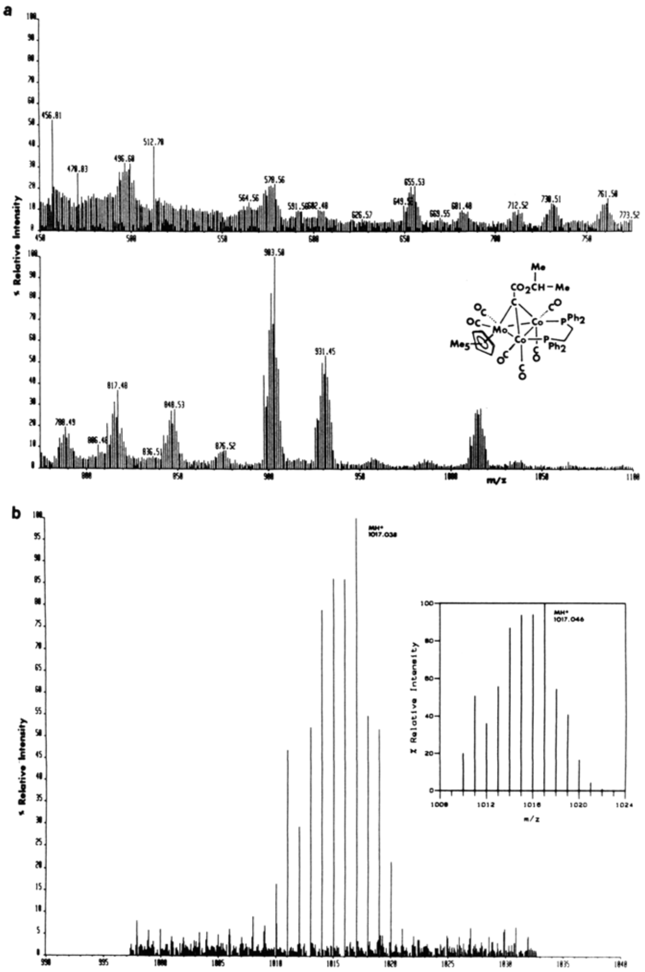

Figure 3. (a) The FAB mass spectrum of **5**. (b) Expansion of the high mass region together with the simulated spectrum in which the M^+:MH^+ ratio is 0.94:1.

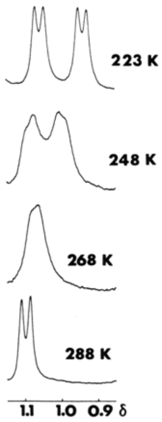

Figure 4. Variable-temperature 250-MHz ^1H NMR spectra of the methyl region of $Co_3(CO)_7$(arphos)CCO_2CHMe_2 (**4**).

than the M^+ ion, and the peaks had to be deconvoluted. Figure 3 also shows the simulated spectrum of these overlapping peaks, and the agreement is excellent.

The ^1H and ^{13}C NMR spectra of the clusters **3** through **6** have been recorded at 9.4 T (400 MHz for ^1H; 100.6 MHz for ^{13}C). As a probe for chirality, an isopropyl substituent was incorporated into the alkylidyne fragment. Since the methyl groups are potentially diastereotopic, they serve to detect racemization on the NMR time scale. Figure 4 shows the variable-temperature ^1H NMR spectrum of the arphos–tricobalt complex **4**; it is apparent that the diastereotopic methyl groups are equilibrated at higher temperatures, indicating that rapid interconversion of enantiomers occurs on the NMR time scale. With use of both the ^1H and ^{13}C spectra, $\Delta G^{\ddagger}$ for this process was evaluated as 13.1 ± 0.5 kcal/mol.

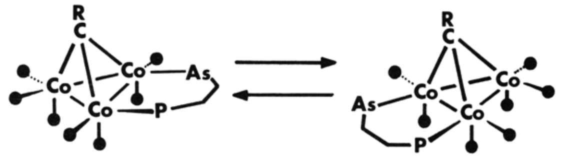

Figure 5. Interconversion of the enantiomers of **4** via arsenic migration.

Because of the low solubility of this and other arphos complexes, it was necessary to enrich the carbonyls to the extent of 30–35% in ^{13}CO. We were thus able to obtain satisfactory variable-temperature NMR spectra for the metal carbonyl resonances. At the lowest temperature attainable, 183 K, the spectrum exhibited a 1:1:2:3 carbonyl pattern which, upon raising the temperature, gradually coalesced to give a single peak. Similar behavior was observed for the analogous diphos–tricobalt complex **3** except that this time the limiting spectrum revealed a 2:2:3 carbonyl pattern corresponding to a $Co(CO)_3$ moiety and the axial and equatorial carbonyls on the $Co(CO)_2P$ fragments. Again, the peaks coalesced as the temperature was raised, and the barrier was measured to be 10.4 ± 0.5 kcal/mol. It is clear that carbonyl exchange in both **3** and **4** occurs much more rapidly than does racemization. Carbonyl scrambling does not, of course, racemize the cluster.

The mechanism by which the chiral complex **4** undergoes racemization is of interest since several processes are potentially viable. One could envisage formal rotation of the RC–$Co(CO)_3$ vector relative to the AsCo–CoP vector. We have discussed such a process as the possible mode of racemization of **1**, but the calculated[12] and experimentally measured[13] barriers are high—of the order of 20–25 kcal/mol! Since **4** racemizes via a process with a barrier roughly half this value, it is unlikely that such a mechanism is operating in this case. More reasonable, perhaps, is the migration of one terminus of the arphos ligand from one cobalt atom to another as depicted in Figure 5. Such a process would also require concomitant migration of the carbonyl ligands; we shall return to this point presently.

Of particular relevance to the present problem is the observation of Robinson et al. that, although a carbonyl group in $RCCo_3(CO)_9$ clusters is readily replaced by a phosphine ligand, arsines bind only weakly. Thus, in $PhCCo_3(CO)_8AsPh_3$, the osmometrically determined molecular weight in solution was always low, indicating that ligand dissociation was occurring.[14] Furthermore, in the reaction between $ClCCo_3(CO)_9$ and Ph_3As, the product contains no arsenic; instead, chlorine is abstracted and $(OC)_9Co_3C$–$CCo_3(CO)_9$ is formed. It is, therefore, not an unreasonable assumption that the weakest bond is the cobalt–arsenic bond and that an intermediate involving a dangling monodentate arphos ligand is implicated. One should note, however, that mere detachment of the arsenic atom from cobalt (accompanied by rapid carbonyl migration) is insufficient in itself to racemize the cluster. A crucial step must be the rotation of the $Co(CO)_2P$ vertex so as to position the phosphorus axially, as in **10**; at this juncture the effective point group becomes C_s and the diastereotopic character of the isopropyl methyls is lost.

---

[12] Hoffmann, R.; Hoffman, D., personal communication.

[13] Jaouen, G.; Marinetti, A.; Saillard, J.-Y.; Sayer, B. G.; McGlinchey, M. J. *Organometallics* **1982**, *1*, 225.

[14] Matheson, T. W .; Robinson, B. H.; Tham, W. S. *J. Chem. Soc. A* **1971**, 1457.

Table III. Selected Interatomic Distances (Å) and Angles (deg)

Bond Distances					
Co(1)-Co(2)	2.500 (3)	Co(2)-Co(3)	2.464 (3)	Co(3)-Co(1)	2.473 (3)
Co(1)-C(8)	1.87 (1)	Co(2)-C(8)	1.87 (1)	Co(3)-C(8)	1.93 (1)
Co(1)-As(P)	2.272 (3)	Co(2)-P(As)	2.229 (3)	Co(1)-C(1)	1.75 (2)
Co(1)-C(2)	1.78 (2)	Co(2)-C(3)	1.68 (2)	Co(2)-C(4)	1.77 (2)
Co(3)-C(5)	1.75 (2)	Co(3)-C(6)	1.76 (2)	Co(3)-C(7)	1.80 (2)
O(1)-O(1)	1.14 (2)	C(2)-O(2)	1.13 (2)	C(3)-O(3)	1.20 (2)
C(4)-O(4)	1.17 (2)	C(5)-O(5)	1.14 (2)	C(6)-O(6)	1.19 (2)
C(7)-O(7)	1.17 (2)	As(P)-C(13)	1.96 (1)	C(13)-C(14)	1.53 (2)
C(14)-P(As)	1.88 (2)	As(P)-C(21)	1.91 (2)	As(P)-C(31)	1.91 (2)
P(As)-C(4)	1.90 (2)	P(As)-C(51)	1.86 (2)	C(8)-C(9)	1.47 (2)
O(8)-C(9)	1.21 (2)	C(9)-O(9)	1.34 (2)	O(9)-C(10)	1.54 (3)
C(10)-C(11)	1.46 (3)	C(10)-C(12)	1.55 (4)		
Bond Angles					
Co(1)-Co(2)-Co(3)	59.8 (1)	Co(2)-Co(3)-Co(1)	60.9 (1)	Co(3)-Co(1)-Co(2)	59.4 (1)
Co(1)-C(8)-Co(2)	83.9 (6)	Co(1)-C(8)-Co(3)	81.2 (5)	Co(2)-C(8)-Co(3)	81.0 (5)
C(8)-Co(1)-Co(2)	48.9 (4)	C(8)-Co(1)-Co(3)	50.3 (4)	Co(8)-Co(2)-Co(1)	48.2 (4)
C(8)-Co(2)-Co(3)	50.5 (4)	C(8)-Co(3)-Co(2)	48.5 (4)	C(8)-Co(3)-Co(1)	48.5 (4)
C(8)-Co(1)-C(1)	98.1 (7)	C(8)-Co(2)-C(3)	112.0 (8)	C(8)-Co(3)-C(5)	103.2 (8)
C(8)-Co(1)-C(2)	146.0 (7)	C(8)-Co(2)-Co(4)	135.8 (7)	C(8)-Co(3)-C(6)	139.3 (8)
C(8)-Co(1)-As(P)	104.2 (4)	C(8)-Co(2)-P(As)	107.0 (4)	C(8)-Co(3)-C(7)	100.2 (7)
Co(2)-Co(1)-C(1)	145.7 (5)	Co(1)-Co(2)-Co(3)	59.8 (1)	Co(1)-Co(3)-C(5)	95.3 (6)
Co(2)-Co(1)-C(2)	105.5 (6)	Co(1)-Co(2)-C(4)	89.3 (6)	Co(1)-Co(3)-C(6)	101.6 (7)
Co(2)-Co(1)-As(P)	99.2 (1)	Co(1)-Co(2)-P(As)	111.8 (1)	Co(1)-Co(3)-C(7)	148.7 (6)
Co(3)-Co(1)-C(1)	96.9 (5)	Co(3)-Co(2)-C(3)	91.6 (6)	Co(2)-Co(3)-C(5)	150.5 (7)
Co(3)-Co(1)-C(2)	98.9 (6)	Co(3)-Co(2)-C(4)	102.4 (6)	Co(2)-Co(3)-C(6)	95.4 (6)
Co(3)-Co(1)-As(P)	153.4 (1)	Co(3)-Co(2)-P(As)	156.8 (1)	Co(2)-Co(3)-C(7)	99.2 (6)
C(1)-Co(1)-C(2)	102.4 (8)	C(3)-Co(2)-C(4)	101.5 (9)	C(5)-Co(3)-C(6)	107.0 (9)
C(1)-Co(1)-As(P)	94.0 (5)	C(3)-Co(2)-P(As)	93.1 (6)	C(5)-Co(3)-C(7)	93.7 (9)
C(2)-Co(1)-As(P)	102.4 (6)	C(4)-Co(2)-P(As)	98.8 (6)	C(6)-Co(3)-C(7)	104.3 (9)
Co(1)-C(1)-O(1)	175.4	C(1)-C(2)-O(1)	173 (2)	Co(1)-As(P)-C(13)	120.4 (4)
Co(1)-As(P)-C(21)	119.5	Co(1)-As(P)-C(31)	113.6 (5)	C(13)-As(P)-C(21)	97.8 (6)
C(13)-As(P)-C(31)	100.1 (6)	C(21)-As(P)-C(31)	102.1 (7)	As(P)-C(13)-C(14)	111 (1)
C(13)-C(14)-P(As)	112 (1)	Co(2)-P(As)-C(14)	119.6 (5)	Co(2)-P(As)-C(41)	117.4 (5)
Co(2)-P(As)-C(51)	110.9 (5)	C(14)-P(As)-C(41)	101.6 (7)	C(14)-P(As)-C(51)	102.7 (7)
C(41)-P(As)-C(51)	102.3 (7)	Co(2)-C(3)-O(3)	177 (2)	Co(2)-C(4)-O(4)	177 (2)
Co(3)-C(5)-O(5)	178 (2)	Co(3)-C(6)-O(6)	176 (2)	Co(3)-C(7)-O(7)	177 (2)
Co(1)-C(8)-C(9)	129 (1)	Co(2)-C(8)-C(9)	136 (1)	Co(3)-C(8)-C(9)	126 (1)
C(8)-C(9)-O(8)	126 (1)	C(8)-C(9)-O(9)	114 (1)	O(8)-C(9)-O(9)	120 (1)
C(9)-O(9)-C(10)	119 (2)	O(9)-C(10)-C(11)	99 (1)	O(9)-C(10)-C(12)	101 (2)
C(11)-C(10)-C(12)	111 (2)				

Had the ground-state geometry of the molecule been a diaxial arrangement for the chelate, the racemization process would presumably have been even more facile.

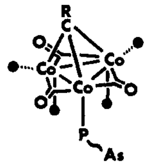

10

In support of this postulate, whereby cobalt–arsenic bond cleavage is favored over cobalt–phosphorus fragmentation, we note the different behavior of the methylene protons in the arphos and diphos complexes. One might have anticipated that the four methylene protons in the backbone of the arphos chain in 4 would be magnetically nonequivalent; they are differentiated not only by their proximity to either phosphorus or arsenic but also by their exo or endo orientation with respect to the cluster. This prediction would have been correct, and, at low temperature, four proton environments are observed. However, as shown in Figure 6, rapid racemization equilibrates the exo and endo positions and the methylenes are differentiated solely by the identity of their group V (15[32]) neighbor. Thus, only two methylene environments remain at high temperature. In contrast, the diphos complex shows two methylene signals at all temperatures, showing that interconversion of the exo and endo protons does not occur. As pointed out earlier, the instantaneous structure of this complex must be asymmetric because of the half-chair conformation of the chelate ring. However, the interconversion of the enantiomers must be rapid on the NMR time scale since not only do we see two (rather than four) methylene environments but also the isopropyl methyls remain equivalent. In this connection, it has been reported[15] that in $Ru_3(CO)_{10}$(dppm) (11) interconversion

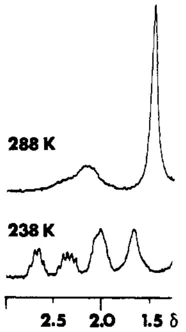

Figure 6. Variable-temperature 250-MHz ^1H NMR spectra of the methylene protons of the arphos ligand in 4.

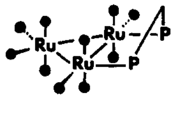

11

---

(15) Cotton, F. A.; Hanson, B. E. *Inorg. Chem.* 1977, *16*, 3369.

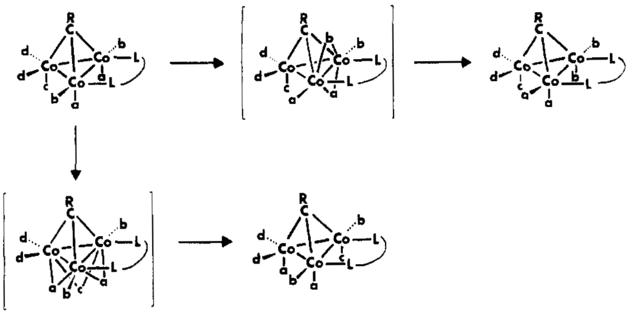

Figure 7. Possible mechanisms to account for carbonyl scrambling.

of the two envelope conformations is apparently sufficiently rapid to render the axial carbonyls equivalent on the NMR time scale. We note also that for the tricobalt–dppm complex 9 the authors comment[9a] that the methylene protons are nonequivalent; of course, rapid flipping of the chelate envelope would not interconvert these proton environments which would remain different—even in the diaxial isomer!

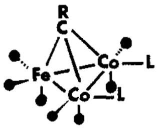

12 L = CO
13 L—L = dppm

As mentioned previously, it is clear from the variable-temperature ^{13}C NMR spectra that the carbonyls scramble much more rapidly than racemization occurs since the former process has a markedly lower barrier. Indeed, carbonyl scrambling over triangular faces of metals is a well-studied phenomenon;[16] and several close analogues of the present system are known.[17] We note initially that Aime and co-workers[18] were able to freeze out localized rotation of the $Fe(CO)_3$ group, but not of the $Co(CO)_3$ moieties, in 12. The 1:2 carbonyl pattern showed that the axial ligand was the more deshielded, and the other assignments were made on this basis. Although internuclear carbonyl scrambling was observed in 12 (leading ultimately to a single peak), the dppm analogue 13 exhibited only localized $Fe(CO)_3$ rotation and the axial and equatorial carbonyls on cobalt remained distinct. In contrast, globalized carbonyl exchange in 3 is rapid and can be simulated as one process with $\Delta G^{\ddagger} = 10.4 \pm 0.5$ kcal/mol. Since the merry-go-round process[19] involving six approximately coplanar equatorial carbonyls is blocked by the presence of the diphos ligand, we sought an analogy in the proposals of Cotton and Hanson[15] with respect to complex 11. They suggested that the six terminal carbonyls bonded to the phosphorus-bearing ruthenium atoms could migrate over an elliptical planar surface presumably via a transition state possessing two bridging and four terminal carbonyl ligands. Likewise, as shown in Figure 7, in molecules 3 or 4 one could envisage interconversion of the CO(a) and CO(b) environments by migration over an elliptical conoidal surface. In 11 the barrier to migration of the axial carbonyls about a cylindrical surface is high, whereas it is known that pseudoaxial carbonyls positioned on a conical surface migrate readily. Typically, in Shapley's $Cp_3Rh_3(\mu\text{-}CO)_3$ molecule (14) the bridging carbonyls couple equivalently to all three ^{103}Rh nuclei at elevated temperature.[20] If such a process were operative in 3, the CO(a) and CO(c) environments would be interconverted. The two migration processes outlined above (which apparently have similar barriers), in conjunction with the rapid localized $Co(CO)_3$ rotation, would allow each carbonyl ready access to all available sites.

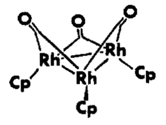

14

Since the tricobalt–arphos complex 4 rapidly loses its stereochemical integrity and is effectively achiral on the chemical time scale, it was decided to incorporate the chelating ligands into $Cp^*MoCo_2(CO)_8CR$ in which it was hoped the bidentate groups would bond only to cobalt. Crystallographic data on the $(C_5H_5)MCo_2(CO)_8CR$ (M = Mo, W) complexes indicated that, at least in the solid state, the molecules possessed a molecular mirror plane and that all the carbonyls were bonded terminally.[21,22] However, Stone has marshalled convincing arguments that in solution several isomers possessing bridging or semibridging carbonyls can coexist. Furthermore, it was tentatively proposed that the dppm derivative might adopt structure 15 in solution.[22]

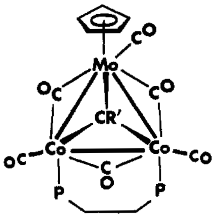

15

The recent establishment of the dppm ligand as an equatorial substituent in 9 prompts us to report the results of a variable-temperature ^{13}C NMR study on ^{13}CO-enriched samples of $(C_5Me_5)Mo(CO)_2Co_2(CO)_6CCO_2$-*i*-Pr (16) and its diphos and arphos derivatives 5 and 6. The ambient-temperature ^{13}C NMR spectrum of 16 gave only a single line in the carbonyl region as anticipated from Stone's results. Upon cooling, however, there appeared peaks at 235 and 200 ppm in a 1:3 ratio appropriate for terminal carbonyls bonded to molybdenum and cobalt, respectively. Further cooling did not freeze out the axial and equatorial exchange at cobalt but rather led to the appearance of another set of peaks in a 1:3 ratio, as shown in Figure 8. Clearly, at least two isomers are detectable and undergo slow interconversion at low temperature. One might speculate that this observation is rationalizable in terms of hindered rotation of the $Cp^*Mo(CO)_2$ vertex relative to the Co_2C triangular face as in Figure 9. Similar phenomena have been discussed by Cotton in the case of Mo_2C_2 tetrahedra[23] and also by Stone for a trigonal bipyramidal closo $MoFe_2C_2$ system.[24] It seems probable that

---

(16) (a) Evans, J. *Adv. Organomet. Chem.* **1977**, *16*, 319. (b) Band, E.; Muetterties, E. L. *Chem. Rev.* **1978**, *78*, 639.

(17) Matheson, T. W.; Robinson, B. H. *J. Organomet. Chem.* **1975**, *88*, 367.

(18) Aime, S.; Milone, L.; Rossetti, R.; Stanghellini, P. L. *Inorg. Chim. Acta* **1977**, *25*, 103.

(19) We assume, as did Cotton and Hanson, that the chelating ligand remains in the diequatorial configuration.

(20) Lawson, R. J.; Shapley, J. R. *J. Am. Chem. Soc.* **1976**, *98*, 7433.

(21) Beurich, H.; Vahrenkamp, H. *Angew. Chem., Int. Ed. Engl.* **1978**, *17*, 863.

(22) Chetcuti, M. J.; Chetcuti, P. A. M.; Jeffery, J. C.; Mills, R. M.; Mitrprachachon, P.; Pickering, S. J.; Stone, F. G. A.; Woodward, P. *J. Chem. Soc., Dalton Trans.* **1982**, 699.

(23) Bailey, W. I., Jr.; Chisholm, M. H.; Cotton, F. A.; Rankel, L. A. *J. Am. Chem. Soc.* **1978**, *100*, 5764.

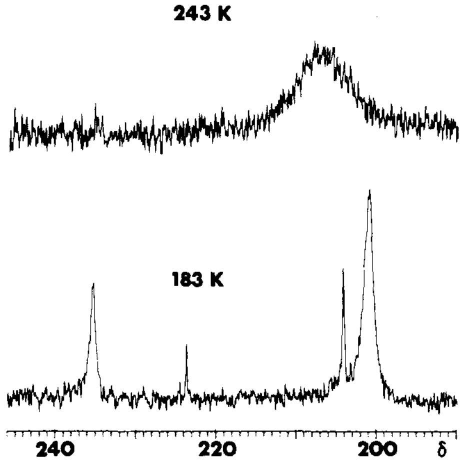

Figure 8. Variable-temperature 100.617-MHz ^{13}C NMR spectra of the metal carbonyl region of $(C_5Me_5)MoCo_2(CO)_8CCO_2CHMe_2$ (**16**).

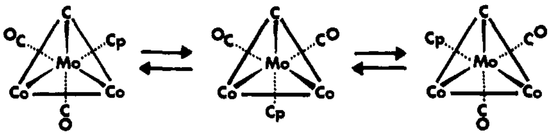

Figure 9. Rotation of a $Cp^*Mo(CO)_2$ vertex relative to a Co_2C triangular face.

one of the rotamers has semibridging carbonyls. Currently we are investigating this equilibrium in more detail, and it will be the subject of a future report.

The ^{31}P NMR spectrum of the $MoCo_2$ cluster **5** shows a single phosphorus environment at a shift indicative of bonding solely to cobalt. In the 100-MHz ^{13}C NMR spectrum at 273 K one sees three equally intense carbonyl resonances at 228, 213, and 209 ppm that are assigned to terminal sites on molybdenum and axial and equatorial positions on cobalt, respectively. We thus favor structure **5** as the predominant isomer in solution rather than the triply carbonyl bridged isomer **15** which had been tentatively proposed previously.[22] Further cooling (see Figure 10) splits the resonance assigned[25] to the equatorial carbonyls on cobalt; the barriers to coalescence are 9.4 ± 0.6 kcal/mol for this latter equatorial carbonyl interconversion and 16.5 ± 0.6 kcal/mol for the process which scrambles the cobalt- and molybdenum-bonded carbonyl ligands. This high-energy exchange phenomenon can only be seen at 333 K on a low-field spectrometer (^1H at 80 MHz; ^{13}C at 20.115 MHz).

The mechanisms of intermetallic carbonyl migration may well parallel those proposed for the tricobalt complex **3**, but this would require that the $Cp^*Mo(CO)_2$ vertex rotate, or at least oscillate, so as to place the carbonyls in favorable positions for bridging and ultimately for transfer to the neighboring cobalt atom. However, the nonequivalence of the equatorial cobalt carbonyls at low temperature suggests that the mirror symmetry of the molecule has been broken, thus rendering the molecule chiral. This is also reflected in the splitting of the isopropyl methyl groups at low temperature. While it is undoubtedly true that freezing the half-chair to half-chair interconversions of the chelate ring would generate molecules of C_1 symmetry, this barrier is almost certainly considerably lower

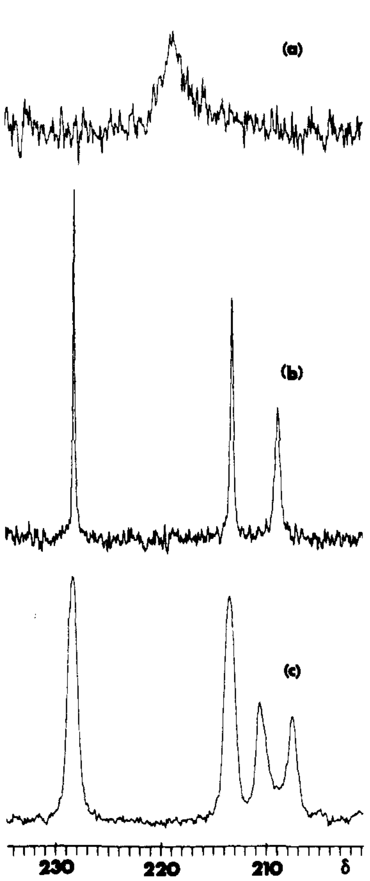

Figure 10. ^{13}C NMR spectra of the metal carbonyl region of $(C_5Me_5)MoCo_2(CO)_6(diphos)CCO_2CHMe_2$ (**5**). (a) At 353 K, 20.115 MHz; (b) at 233 K, 100.617 MHz; (c) at 198 K, 100.617 MHz.

than the 9.4 kcal/mol value observed for the equatorial carbonyl exchange. Furthermore, if this were to be the origin of the chirality, similar behavior would have been expected for the tricobalt analogue **3** but such is not the case. We note, however, that this barrier of 9.4 kcal/mol falls precisely in the range reported by Cotton for $CpMo(CO)_2$ oscillation in the tetrahedral dimolybdenum–alkyne complexes mentioned above.[23] One might therefore suspect that the nonequivalence of the equatorial cobalt carbonyls arises as a consequence of a preferred conformation of the molybdenum vertex such that the cyclopentadienyl ligand is not symmetrically disposed with respect to the plane containing the molybdenum and carbynyl carbon atoms and bisecting the Co–Co bond. Clearly, X-ray crystallographic data would be valuable in this context.

The Co_2Mo–arphos complex **6** likewise shows a single carbonyl resonance at high temperature that decoalesces to give two molybdenum carbonyl resonances and, of course, splits the cobalt carbonyls into axial and equatorial environments that are further differentiated by their proximity to either phosphorus or arsenic. The isopropyl methyl groups are diastereotopic at all temperatures showing that, even if cobalt–arsenic bond scission occurs, the molecule does not racemize. Indeed, at low temperatures, several new methyl and carbonyl resonances appear; presumably, this is attributable to slowed rotation of the molybdenum vertex that consequently freezes out a multitude of diastereomers.

To conclude, in these tetrahedral trimetallic clusters, intermetallic carbonyl scrambling has a low barrier (~10–11 kcal/mol) while in the arphos complex **4**, migration of an arsenic terminus racemises the molecule; this latter process has an activation energy of ~13 kcal/mol. Further

---

[24] Green, M.; Marsden, K.; Salter, I. D.; Stone, F. G. A.; Woodward, P. *J. Chem. Soc., Chem. Commun.* **1983**, 446.

[25] We here follow the pattern established by Aime et al. for an $Fe(CO)_3$ moiety (ref 18) that the axial carbonyls are less shielded than their equatorial partners.

studies are in progress using solid-state ^{13}C NMR spectroscopy to elucidate the mechanisms of carbonyl exchange.

Experimental Section

All preparations were carried out under an atmosphere of dry nitrogen. Solvents were dried according to standard procedures.[26] Infrared spectra were recorded on a Perkin-Elmer 283 instrument using either KBr solution cells or NaCl plates. NMR spectra were obtained by using a Bruker WM 400, WM 250, or WP 80 spectrometer. Variable-temperature spectra were simulated by using the program DNMR3.[27] ^{1}H and ^{13}C chemical shifts are reported relative to tetramethylsilane; ^{31}P chemical shifts are quoted relative to 85% H_3PO_4. Electron-impact mass spectra were recorded by using a VG-7070F mass spectrometer equipped with a VG 7035 data system. Fast atom bombardment (FAB) mass spectra were obtained on a VG analytical ZAB-SE spectrometer with an accelerating potential of 8 kV and a resolving power of 10 000. Thioglycerol was used as the sample matrix and Xe as the bombarding gas. The cluster pattern is a combination of M^+ and $(M + H)^+$ and so needed to be deconvoluted. Elemental composition is confirmed by the accurate mass measurement on the molecular ion. Microanalytical data are from Guelph Chemical Laboratories, Guelph, Ontario.

Collection of the Crystal Data. A black platelike crystal was used for the X-ray studies. Precession photographs showed it was orthorhombic and unit cell parameters were obtained from a least-squares fit of χ, ϕ, and δ for 15 reflections in the range $18.1° < 2\theta < 24°$. All measurements were made on a Syntex P2 diffractometer with use of graphite-monochromated Mo Kα radiation ($\lambda = 0.71069$ Å). Crystal data and other numbers related to data collection are summarized in Table I. The density was obtained by flotation. Intensities were measured with a coupled θ (crystal)–2θ (counter) scan. The methods of selection of scan rates and initial data treatment have been described.[28] Data collection over $h,k,+l$ resulted in 7436 reflections. After reduction and averaging of redundant data (agreement factor or $R_{\mathrm{merg}} = 0.026$) there were 4354 independent reflections of $I > 0$ and 2317 reflections with $I > 3\sigma$. Two standard reflections measured every 48 reflections showed only 1.2% decay over the course of data collection. Corrections were made for Lorentz–polarization effects, but not for absorption. This will introduce a maximum error in F_o of 9%.

Solution of the Structure. The phases were determined by direct methods with use of 50 reflections with $E > |1.28|$ and 12 sets of starting phases. The cobalt, phosphorus, and arsenic atoms were found in the subsequent E map. A series of full-matrix least-squares refinements, followed by three-dimensional electron difference syntheses, revealed all the non-hydrogen atoms. No attempt was made to find the hydrogen atoms. The temperature factors of the arsenic and phosphorus atoms were unsatisfactory, and it was apparent that the phosphine–arsine ligand was disordered. Occupancy of the phosphorus and arsenic positions was included in the refinement, with the restriction that the occupancies of phosphorus plus arsenic on each site equaled 1.0, and the total phosphorus and total arsenic were both 1.0. Temperature factors of the Co, P, and As atoms were made anisotropic, and further full-matrix least-squares refinement that minimized $\sum w(|F_o| - |F_c|)^2$ was terminated when the shift/error ratio was <0.02. Corrections were made for secondary extinction by the method in SHELX.[29] Throughout the refinement, scattering curves were taken from ref 30, and anomalous dispersion corrections from ref 31 were applied to the curves for Co, P, and As.

The quality of the crystal was not high, and the large number of light atoms also contributed to problems of structure solution, leading to a high percentage of unobserved reflections. In an attempt to include weak reflections in the structure solution ($I > 0$) the solution refined to $R_1 = 0.138$ and $R_2 = 0.141$. Use of only observed reflections ($I > 3\sigma$) gave agreement factors of $R_1 = 0.075$ and $R_2 = 0.092$.

$Co_3(CO)_9CCO_2CH(CH_3)_2$ (17). Following the procedure of Seyferth,[3] $Co_2(CO)_8$ (7.26 g, 21.2 mmol) and $CCl_3CO_2CH(CH_3)_2$(2.42 g, 11.8 mmol) were heated under reflux in tetrahydrofuran (75 cm^3) for 3.5 h. After the mixture was cooled to room temperature and filtered to remove the cobalt salts, the filtrate was evaporated to dryness and the crude product was recrystallized from hexane to give **17** (4.17 g, 7.89 mmol; 66%): mp 64 °C (lit.[3] 64–65 °C); IR (C_6H_{12}) ν_{CO} 2100 (w), 2055 (s), 2035 (s), 1687 (ester) cm^{-1}; ^{1}H NMR (WM-250; C_6D_6) δ 5.22 (septet, $J_{HH} = 6.2$ Hz, 1 H), 1.23 (d, 6 H); ^{13}C NMR (WM-400; CD_2Cl_2) δ 198.8 (CO's) 69.7 (CH), 21.7 (CH_3).

$[C_5(CH_3)_5]MoCo_2(CO)_8CCO_2CH(CH_3)_2$ (16). $[C_5(CH_3)_5Mo(CO)_3]_2$ (0.21 g, 0.33 mmol) and **17** (0.34 g, 0.66 mmol) were heated under reflux in tetrahydrofuran (50 cm^3) for 18 h. Progress of the reaction was followed by TLC on Kieselgel (eluent, ether/petroleum ether, 15/85) showing a purple-brown spot, **17** (R_f 0.76), and a green spot, **16** (R_f 0.37). After filtration and removal of solvent, chromatography on silica gel using ether/petroleum ether, 15/85, yielded green crystals of **16** (0.067 g, 0.1 mmol; 30%): mp 135 °C; IR (C_6H_{12}) ν_{CO} 2090 (s), 2055 (s), 2040 (s), 2020 (m), 2010 (m), 1935 (m), 1880 (m), 1673 (ester) cm^{-1}; ^{1}H NMR (WM-250; C_6D_6) δ 5.2 (septet, $J_{HH} = 6.2$ Hz, 1 H), 1.79 (s, 15 H), 1.33 (d, 6 H); ^{13}C NMR (WM-400; CD_2Cl_2; 183 K) δ 235.0, 223.5 (Mo–CO's; 8:1 ratio), 204.1, 200.9 (Co–CO's; 3:24 ratio), 105.7 (Cp–C), 21.8 (CH_3) 9.8 (Cp–CH_3). FAB mass spectrum: m/z (%) 674 (8) $C_{23}H_{22}Co_2MoO_{10}$ (M^+); 646 (2) $(M - CO)^+$; 618 (10) $(M - 2CO)^+$; 590 (9) $(M - 3CO)^+$; 562 (7) $(M - 4CO)^+$; 534 (7) $(M - 5CO)^+$; 506 (10) $(M - 6CO)^+$; 478 (6) $(M - 7CO)^+$; 450 (15) $(M - 8CO)^+$; 135 (100) $C_{10}H_{15}^+$. Molybdenum-containing peak masses are calculated on only the basis of ^{98}Mo, but all such ions give peak envelopes showing the correct isotopic distribution. Anal. Calcd for $C_{23}H_{22}Co_2MoO_{10}$: C, 41.09; H, 3.30. Found: C, 41.19; H, 3.37.

$Co_3(CO)_7CCO_2CH(CH_3)_2(Ph_2PCH_2CH_2PPh_2)$ (3). A solution of **17** (0.34 g, 0.66 mmol) and diphos (0.26 g, 0.66 mmol) in THF (35 cm^3) was stirred at ambient temperature for 45 min. The progress of the reaction was followed by TLC (eluent, ether/petroleum ether, 15/85) which revealed the formation of **3** (R_f 0.14) as a green spot. Chromatography on silica gel (eluent, ether/hexane, 10/90) gave dark green crystals of **3** (0.19 g, 0.22 mmol; 33%): mp 123 °C; IR (C_6H_{12}) ν_{CO} 2085 (m), 2075 (s), 2050 (m), 2030 (s), 2020 (s), 1980 (m), 1650 (ester) cm^{-1}; ^{1}H NMR (WM-250; CD_2Cl_2), δ 7.7–7.3 (m, 20 H), 4.63 (septet, $J_{HH} = 6.4$ Hz, 1 H), 2.47 (m, 2 H), 2.06 (m, 2 H), 1.14 (d, 6 H); ^{13}C NMR (WM-400; CD_2Cl_2; 223 K) δ 210.2 (2 CO), 204.3 (2 CO), 202.5 (3 CO), 181.7 (C=O), 136.2, 131.8, 130.3, 128.6 (Ph), 68.2 (CH), 24.1 (d, $J_{CP} = 24$ Hz, CH_2–P), 21.6 (CH_3); ^{31}P NMR (C_6D_6) 42.0 ppm. FAB mass spectrum: m/z (%) 870 (28) $C_{38}H_{31}Co_3O_9P_2$ (M^+); 842 (22) $(M - CO)^+$; 786 (69) $(M - 3CO)^+$; 758 (35) $(M - 4CO)^+$; 730 (23) $(M - 5CO)^+$; 702 (54) $(M - 6CO)^+$; 674 (52) $(M - 7CO)^+$; 616 (80) $C_{28}H_{25}Co_3OP_2$; 588 (90) $C_{27}H_{25}Co_3P_2$; 431 (100) $C_{16}H_{15}Co_3P$. Anal. Calcd for $C_{38}H_{31}Co_3O_9P_2$: C, 52.44; H, 3.59. Found: C, 52.69; H, 3.71.

$Co_3(CO)_7CCO_2CH(CH_3)_2(Ph_2AsCH_2CH_2PPh_2)$ (4). A solution of **17** (0.26 g, 0.50 mmol) and arphos (0.22 g, 0.50 mmol) in THF (50 cm^3) was heated under reflux for 1.5 h. Chromatography on silica gel (eluent ether/hexane, 10/90) gave dark purple crystals

---

(26) Perrin, D. D.; Perrin, D. R. *Purification of Laboratory Chemicals*; Pergamon: New York, 1980.

(27) Kleier, D. A.; Binsch, G. *QCPE* **1969**, *No. 165*.

(28) (a) Hughes, R. P.; Krishnamachari, N.; Lock, C. J. L.; Powell, J.; Turner, G. *Inorg. Chem.* **1977**, *16*, 314. (b) Lippert, B.; Lock, C. J. L.; Rosenberg, B.; Zvagulis, M. *Inorg. Chem.* **1977**, *16*, 1525.

(29) All computations were carried out on CYBER 170/730 or 815 computers. Programs used for initial data treatment were from the XRAY76 package (Stewart, J. M. Technical Report TR-446; University of Maryland: College Park, MD, 1976). The structure was solved with SHELX (Sheldrick, G. M., Cambridge University, Cambridge, England, 1976). Planes were calculated with use of NRC-22 (Ahmed, M. R.; Pippy, M. E., National Research Council of Canada, Ottawa, Canada, 1978). Diagrams were prepared from ORTEP II (Johnson, C. K. Report ORNL-5138; Oak Ridge National Laboratory: Oak Ridge, TN, 1976).

(30) Cromer, D. T.; Waber, J. T. *International Tables for X-ray Crystallography*; Ibers, J. A., Hamilton, W. C., Eds.; Kynoch Press: Birmingham, England, 1974; Vol. IV, Table 2.2B, pp 99–101.

(31) Cromer, D. T. Ref 29, Table 2.3.1, pp 149–150.

(32) In this paper the periodic group notation in parentheses is in accord with recent actions by IUPAC and ACS nomenclature committees. A and B notation is eliminated because of wide confusion. Groups IA and IIA become groups 1 and 2. The d-transition elements comprise groups 3 through 12, and the p-block elements comprise groups 13 through 18. (Note that the former Roman number designation is preserved in the last digit of the new numbering: e.g., III → 3 and 13.)

of 4 (0.25 g, 0.27 mmol; 54%): mp 176 °C; IR (C_6H_{12}) ν_{CO} 2060 (s), 2015 (s), 2005 (s), 1980 (s), 1955 (m, br), 1650 (ester) cm^{-1}; ^1H NMR (WM-250; CD_2Cl_2; 223 K) δ 7.7–7.3 (m, 20 H), 4.58 (septet, J_{HH} = 6.3 Hz, 1 H), 2.65 (m, 1 H), 2.34 (m, 1 H), 2.01 (m, 1 H), 1.98 (m, 1 H), 1.10 (d, 3 H), 0.99 (d, 3 H); ^{13}C NMR (WM-400; CD_2Cl_2; 183 K) δ 243.1 (apical C), 210.5 (1 CO), 208.8 (1 CO), 203.5 (2 CO), 201.6 (3 CO), 182.2 (C=O), 137.7, 132.1, 130.5, 130.2, 129.2, 129.0 (Ph), 68.5 (CH), 25.4 (d, J_{CP} = 23 Hz, (CH_2–P), 23.1 (CH_2–As), 22.0 (CH_3); ^{31}P NMR (C_6D_6) 47.6 ppm. FAB mass spectrum: *m/z* (%) 914 (28) $C_{38}H_{31}Co_3O_9AsP$ (M^+); 886 (4) (M – CO)$^+$; 858 (4) (M – 2CO)$^+$; 830 (10) (M – 3CO)$^+$; 802 (4) (M – 4CO)$^+$; 774 (8) (M – 5CO)$^+$; 746 (4) (M – 6CO)$^+$; 718 (9) (M – 7CO)$^+$; 660 (14) $C_{28}H_{25}Co_3OAsP$; 632 (17) $C_{27}H_{25}Co_3AsP$; 59 (100) Co. Anal. Calcd for $C_{38}H_{31}AsCo_3O_9P$: C, 49.92; H, 3.36. Found: C, 49.88; H, 3.52.

$[C_5(CH_3)_5]MoCo_2(CO)_6CCO_2CH(CH_3)_2(Ph_2PCH_2CH_2PPh_2)$ (5). As with the synthesis of the tricobalt complex **3**, diphos and **16** in THF gave **5** in 56% yield: mp 117 °C; IR (C_6H_{12}) ν_{CO} 2090 (w), 2050 (m), 2040 (m), 2010 (m), 1990 (s), 1970 (s), 1945 (s), 1920 (w), 1910 (w), 1660 (ester) cm^{-1}; ^1H NMR (WM-250; CD_2Cl_2) δ 7.6–7.3 (m, 20 H), 4.2 (septet, J_{HH} = 6.0 Hz, 1 H), 2.80 (m, 2 H), 2.45 (m, 2 H), 2.04 (s, 15 H), 1.06 (d, 6 H); ^{13}C NMR (WM-400; CD_2Cl_2; 198 K) δ 228.0 (2 CO) (Mo–CO's), 213.2 (2 CO), 210.5 (1 CO), 207.6 (1 CO) (Co–CO's), 133.5, 129.5, 128.3, 127.9 (Ph), 102.0 (Cp–C), 68.2 (CH), 24.1 (d, J_{CP} = 24 Hz) (CH_2–P), 24.1 (CH_3) 11.2 (Cp–CH_3); ^{31}P NMR (C_6D_6) 37.4 ppm. FAB mass spectrum: *m/z* (%) 1016 (28) $C_{47}H_{46}Co_2MoO_8P_2$ (M^+); 988 (4) (M – CO)$^+$; 960 (5) (M – 2CO)$^+$; 932 (53) (M – 3CO)$^+$; 904 (100) (M – 4CO)$^+$; 876 (8) (M – 5CO)$^+$; 848 (28) (M – 6CO)$^+$; 713 (10) (M – 6CO – C_5Me_5)$^+$. Anal. Calcd for $C_{47}H_{46}Co_2MoO_8P_2$: C, 55.64; H, 4.57. Found: C, 55.32; H, 4.81.

$[C_5(CH_3)_5]MoCo_2(CO)_6CCO_2CH(CH_3)_2(Ph_2AsCH_2CH_2PPh_2)$ (6) was prepared analogously to **3**; arphos and **16** in THF gave **6** in 82% yield: mp 105 °C; IR (C_6H_{12}) ν_{CO} 2065 (s), 2020 (s), 2015 (s), 1985 (m), 1655 (ester) cm^{-1}; ^1H NMR (WM-250, CD_2Cl_2) δ 7.7–7.2 (m, 20 H), 4.1 (septet, J_{HH} = 6.2 Hz, 1 H), 3.02 (m, 1 H), 2.65 (m, 1 H), 2.44 (m, 1 H), 2.10 (m, 1 H), 2.05 (s, 15 H), 1.10 (d, 3 H), 1.03 (d, 3 H); ^{13}C NMR (WM-400; CD_2Cl_2; 213 K) δ 228.4 (1 CO), 226.9 (1 CO) (Mo–CO's), 213.1 (2 CO), 208.6 (1 CO), 208.0 (1 CO) (Co–CO's), 132.5, 130.2, 128.3, 127.8 (Ph), 101.7 (Cp–C), 67.4 (CH), 25.3 (d, J_{CP} = 24 Hz, CH_2–P), 21.2 (CH_2–As), 20.9 (CH_3) 11.0 (Cp–CH_3); at 183 K extra CO resonances appear at δ 235.5, 231.5, 209.2, 204.3, 201.0; ^{31}P NMR (C_6D_6) 41.0 ppm. Anal. Calcd for $C_{47}H_{46}AsCo_2MoO_8P$: C, 53.33; H, 4.38. Found: C, 53.40; H, 3.99.

Carbonyl Enrichments. In a typical experiment, **3** (0.1 g, 0.11 mmol) in THF (35 cm^3) was stirred under an atmosphere of ^{13}CO for 48 h. The solvent was removed in vacuo and the product analyzed mass spectrometrically; enrichment was usually of the order 25–30%. On a Bruker WM 400, an acceptable ^{13}C NMR spectrum could be obtained after 100 scans.

Acknowledgment is made to the donors of the Petroleum Research Fund, administered by the American Chemical Society, for partial support of this research. Financial support from the Natural Sciences and Engineering Research Council of Canada is also gratefully acknowledged. G.J. thanks the France–Canada Scientific Exchange Program for a visiting Professorship. K.A.S. and M.M. thank NSERC for graduate fellowships.

Supplementary Material Available: Lists of anisotropic temperature factors and bond lengths and angles within the phenyl rings (2 pages); lists of calculated and observed structure factor amplitudes (25 pages) Ordering information is given on any current masthead page.

Reactions of Acetylenes with the Cationic Bridging Methylidyne Complex $[(C_5H_5)(CO)Fe]_2(\mu\text{-}CO)(\mu\text{-}CH)^+$

Charles P. Casey,* L. Keith Woo, Paul J. Fagan, Robert E. Palermo, and Bruce R. Adams

Department of Chemistry, University of Wisconsin, Madison, Wisconsin 53706

Received June 18, 1986

Reaction of $[(C_5H_5)(CO)Fe]_2(\mu\text{-}CO)(\mu\text{-}CH)^+PF_6^-$ (**1**) with 2-butyne produced $(C_5H_5)_2(CO)Fe_2(\mu\text{-}CO)(\mu\text{-}\eta^1,\eta^4\text{-}CHC(CH_3)C(CH_3)CO)^+PF_6^-$ (**2**) in 76% yield. The structure of **2** was determined by X-ray crystallography: monoclinic space group $P2_1/c$, with cell constants a = 7.576 (3) Å, b = 19.053 (8) Å, c = 13.439 (9) Å, β = 101.03 (4)°, Z = 4, and R = 0.083 and R_w = 0.090 for 1895 reflections with $F_o \geq 3\sigma(F_o)$. **1** reacted regioselectively with phenylacetylene to produce $(C_5H_5)_2(CO)Fe_2(\mu\text{-}CO)(\mu\text{-}\eta^1,\eta^4\text{-}CHCHC(C_6H_5)CO)^+PF_6^-$ (**7**) in 81% yield. The reaction of **1** with *tert*-butylacetylene gave an 88% yield of an 80:20 mixture of $[(C_5H_5)(CO)Fe]_2(\mu\text{-}CO)(\mu\text{-}\eta^1,\eta^2\text{-}CH{=}CHC(CH_3){=}C(CH_3)_2)^+PF_6^-$ (**9-PF$_6$**) and $[(C_5H_5)(CO)Fe]_2(\mu\text{-}CO)(\mu\text{-}\eta^1,\eta^2\text{-}CH{=}C{=}CHC(CH_3)_3)^+PF_6^-$ (**10-PF$_6$**).

Introduction

The cationic diiron bridging methylidyne complex $[(C_5H_5)(CO)Fe]_2(\mu\text{-}CO)(\mu\text{-}CH)^+PF_6^-$ (**1**) is very electrophilic.[1] Nucleophiles such as CO and NMe_3 add to the methylidyne carbon of **1** to form stable 1:1 adducts.[1] The reactions of alkenes with **1**, which lead to either μ-alkylidyne or μ-alkenyl products, are initiated by an interaction of the alkene with the electrophilic methylidyne carbon. For ethylene, monosubstituted alkenes, and isobutylene, the transition state for reaction with **1** involves interaction of the methylidyne carbon with the least substituted alkene carbon and development of partial positive charge at the more substituted alkene carbon. After this rate-determining transition state, a 1,3-hydride shift from the methylidyne carbon to the alkene completes the formation of the μ-alkylidyne product.[2] For some alkenes such as

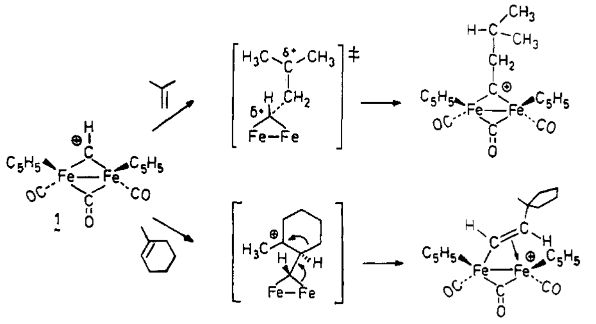

---

[1] Casey, C. P.; Fagan, P. J.; Day, V. W. *J. Am. Chem. Soc.* **1982**, *104*, 7360–7361.